Direct Optical Switching Code-Division Multiple-Access System for Fiber-Optic Radio Highway Networks

Katsutoshi Tsukamoto, *Member, IEEE*, Takeshi Higashino, Takashi Nakanishi, and Shozo Komaki, *Senior Member, IEEE*

Invited Paper

***Abstract*—Recently, microwave photonics techniques have significantly progressed to realize a new type of communication system enhancing the synergetic effect of wireless easy access and photonic broadbandness. This paper describes the concept of radio highway networks configured by radio on fiber links, which are transparent for various types of radio formats. Also as an effective candidate for a multiple-access method of radio signal into the radio highway network, this paper reports direct optical switching code-division multiple-access system and shows its performance theoretically and experimentally.**

***Index Terms*—Microwave photonics, optical code-division multiple access (CDMA), radio highway, radio on fiber.**

I. Introduction

RADIO on fiber (RoF) links have the function of transferring radio signals into remote stations with keeping their radio format, such as radio frequencies, modulation formats, and so on. Consequently, RoF links are considered hopeful candidates for various future cellular access networks, such as next-generation mobile communication systems, road-to-vehicle radio access links in intelligent transport systems (ITS), or distribution systems of cable TV signals. Actually, many systems employing RoF techniques have been developed and used for ITS [1] and mobile communication applications in underground, tunnels, and in buildings that ordinarily become a dead zone for radio signals[2]–[5]. For this purpose, the transmission format in the fiber-optic networks is typically based on analog optical modulation techniques [6]–[12].

However, the technologies for radio access systems continue changing rapidly and many new wireless access systems will appear to satisfy the tremendous increase of users' demands. Since different wireless access services have usually different types of radio signal formats, different types of radio base stations (RBSs) and backbone networks should be segregated according to their services and operators. Consequently, a long time and an excessive investment are necessary to start a new wireless access service or to change its radio format.

In order to solve this problem, the concept of radio highway networks has been proposed, as illustrated in Fig. 1 [11]. The radio access zone architecture employs conventional microcellular or picocellular radio systems. However, the RBS receiving or transmitting radio signals in each radio zone equip only the converter between radio signals and optical signals. The RBS requires neither the modulation functions nor the demodulation functions of radio signals. The radio signals converted into optical signals are transferred via an RoF link with the benefit of its low transmission loss. Therefore, the RoF links can be independent of the radio signals' format and can provide many universal radio access methods. This means that radio highway networks are very flexible to the modification of radio signal formats, the opening of new radio services, or the accommodation of some different types of radio signal formats. A remote central station, called the radio control station (RCS), executes the functions of modulation and demodulation of radio and other controls such as channel allocation, handover processing, and so on. Such concentrated execution of their complicated function provides a much simplified and cost-effective radio access network and promises easy realization of recent advanced demodulation techniques, such as macro diversity, handover control, and interference cancellations.

In order to realize radio highway networks, one subject is which photonic link configuration and multiplexing scheme is suitable. Three topologies become candidates for the RoF link configuration: star, ring, and bus configurations. The latter two can reduce the fiber count; thus they offer cost-effective and quick construction of networks and also easy extension of RBSs. Capabilities are very important in realizing radio highway networks because the density of RBSs increases according to the number of users, and becomes very high in recent micro/picocellular requirements. For indoor use, network flexibility and fiber count reduction are very important matters, because the reinstallation of fibers is wasteful. In employing passive fiber-optic topologies such as passive double star, ring, and bus topologies, another important subject is a photonic access scheme for various types of radio air

Manuscript received April 28, 2003; revised September 2, 2003. This work is supported in part by the Japan Society for the Promotion of Science under Grants-in-Aid for Scientific Research (B) No. 14350202.

The authors are with the Department of Communications Engineering, Graduate School of Engineering, Osaka University, 565-0871 Suita-shi, Japan (e-mail: tukamoto@comm.eng.osaka-u.ac.jp).

Digital Object Identifier 10.1109/JLT.2003.819789

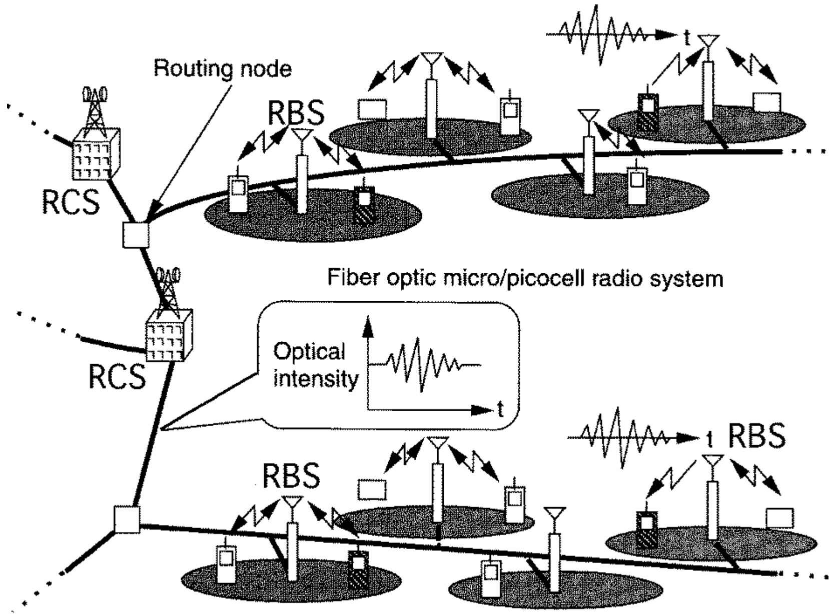

Fig. 1. Concept of radio highway networks.

interfaces. The candidates are subcarrier multiplexing (SCM), time-division multiple access (TDMA), code-division multiple access (CDMA), and wavelength-division multiple (WDM) access. In discussing a suitable photonic multiplexing scheme for radio highway networks, we should make much of the cost efficiency, the ease of use, and the simplicity of network configuration.

As mentioned above, the radio highway networks have the potential to be universally used for different radio services operated by different operators, because the configuration of RBSs and RoF links can be independent of the radio signal formats. Such advanced purpose requires further subjects. The different types of radio services operated by different carriers will need to be delivered to different RCSs in different locations in most cases. This means that the networks should include the routing node that executes routing of radio signals, that is, distinguishing and switching of radio signals. Therefore, in selecting a particular multiplexing scheme, it is also important to make much of the simplicity for the routing of radio signals, and it is desirable that the routing process should be implemented at the optical stages in order to keep its transparency for radio signals.

As a multiple-access method for the radio highway networks, SCMA methods [6], [13] and TDMA methods [14], [15] have often been discussed. The SCMA method exceeds in simplicity and flexibility. However, each radio cell needs a different radio frequency, and optical signal beat noises severely deteriorate the carrier-to-noise ratio (CNR) at the RCS if there are no strict controls of optical wavelengths of laser diodes connected to the RoF link at each RBS. Reference [16] investigates the reduction of optical signal beat noises in the SCM/WDM network. On the other hand, TDMA method is an attractive candidate because no optical beat noises arise and a radio frequency can be reused among several microcells. However, this method needs the time synchronization of the whole system. In the downlink of radio highway networks, for example, the radio or video distribution can be provided by the conventional multiplexing method such as SCMA method. On the other hand, the uplink traffic is not so large in spite of many potential subscribers, but there exist various types of radio signals that have different frequencies and different multiple-access methods. The CDMA method will be another candidate as a multiple-access method for the uplink of radio highway networks. The CDMA method needs the chip syncronization among the used spreading codes. However, its asynchronous access property, flexibility, and transparency for various radio air interfaces are more attractive than SCMA methods and TDMA methods.

It has been necessary to find new optical CDMA methods for radio highway networks from the viewpoints of the flexibility in assigning code sequences and the implementation by RoF links using the optical intensity modulation (IM). The proposed direct optical switching (DOS)-CDMA scheme [17] can be performed only with an optical switch (OSW) at the transmitter and also an OSW, a photodetector (PD), and an electrical bandpass filter (BPF) at the receiver. Therefore, any type of radio signal can be converted into optical IM/CDMA signals. In the DOS-CDMA scheme, multiplexing is performed by randomizing positions of optical pulses at an OSW driven with a pseudonoise (PN) unipolar code sequence such as optical orthogonal code (OOC). Furthermore, when the DOS-CDMA scheme employs the optical polarity reversing correlator (OPRC) to use bipolar PN codes which are usually used in CDMA radio systems, the number of multiplexed radio signals can be increased [18].

This paper describes the principle of our proposed DOS-CDMA scheme, shows some theoretical analysis results of the system performance, and gives the latest experimental results of the received radio signal quality improved by using OPRC. Also, this paper experimentally examines the improvement in carrier-to-(interference plus noise) ratio (CINR) obtained by assigning even weight of a bipolar code to optical intensity pulse for the first time.

The remainder of this paper is composed as follows. Section II describes the principle of the DOS-CDMA for radio highway networks. Section III describes the OPRC for the DOS-CDMA scheme and shows the theoretical analysis results of the carrier-to-interference power ratio (CIR), which show that the OPRC using bipolar PN codes can further improve the number of maximum connected RBSs over the unipolar type correlator using prime codes as one of OOC. Section IV describes some experimental results.

II. Direct Optical Switching CDMA Method

A. Optical CDMA Method

There are two CDMA methods that can be applied for the radio highway network. One is the electrical CDMA and IM method [19], in which radio signals are spectrum-spread in the electrical domain and converted into optical IM signals at the laser diode (LD), and their correlations are performed in the electrical domain after the photodetection at the PD. This method is the most conventional one, but it is difficult to use a chip rate of more than hundreds of megachips per second because of the band limitation of the electrical circuits. As a result, the spreading gain is rather low and the number of multiple-access RBSs is limited.

Another is the optical CDMA method, in which the spectrum-spreading of radio signals and their correlations are performed in the optical domain. The optical CDMA method is more suitable than the conventional electrical CDMA method because various types of radio signals can be multiplexed in optical domain and high processing gains can be gained with ease by using the broad bandwidth of optical devices.

Up to this time, various optical CDMA methods have been studied mainly for digital optical local-area networks. Optical CDMA methods such as using fiber delay lines [20], optical phase masks [21], and coherent optical phase modulations [22] have been proposed. In the optical CDMA method using fiber delay lines, the encoding and the decoding are performed by delaying optical pulses in the time domain. In the optical CDMA method using optical phase masks, the spectral encoding and the decoding are performed by phase-modulating optical pulses in the domain of optical frequency. These methods can be applied for optical digital modulation; however, it is difficult to apply them for multiplexing radio signals for radio highway networks because the networks are configured with analog IM RoF links. Furthermore, these methods lack flexibility in assigning code sequences. The optical coherent CDMA methods use optical phase modulations; therefore, their correlator is quite the same as in the RF spread-spectrum system but needs very complicated and fine narrow-band optical filters, which are very sensitive to temperature changes. On the other hand, the optical CDMA using optical disk patterns has been proposed [23]. However, in this method, the assignment of code sequences is not flexible and the application to radio signals has not been taken into account.

Therefore, it has been necessary to find new optical CDMA methods for radio highway networks from the viewpoints of flexibility in assigning code sequences and the optical CDMA using the optical IM. The proposed DOS-CDMA[17] scheme can be performed only with an OSW at the transmitter, and also an OSW, a PD, and an electrical BPF at the receiver. Consequently, any types of radio signal can be converted into optical IM/CDMA signals. In the DOS-CDMA scheme, the multiplexing is performed by randomizing positions of optical pulses at an OSW driven with a PN code. This is quite different from the random-access discrete address scheme using quantized pulse position modulation [24].

B. Principle of DOS-CDMA Method

The DOS-CDMA scheme uses ON–OFF type switching spectral spreading. Each radio signal received at each RBS is transmitted to an RCS by analog-type optical pulse amplitude modulation (PAM) scheme, and the multiple access among many RBSs is performed by the DOS-CDMA scheme. The regeneration of radio signal is based on the bandpass natural sampling theory [15], [25]. Fig. 2 shows the system model to illustrate the principle of the DOS-CDMA process at the RBS transmitter and the correlating process at the RCS receiver.

At the RBS, a received radio signal is converted into an optical IM signal by modulating LD directly, next sampled at an OSW, which is driven with a certain code sequence $\mathrm{c_k(t)}$, and the output signal of OSW is transmitted to a receiver through optical fiber. At the output of OSW in the transmitter, we can obtain optical PAM/IM signals whose pulses are positioned according to the code pattern of $\mathrm{c_k(t)}$. At the receiver, many PAM/IM signals from many RBSs are correlated with the code sequence $\mathrm{c_k(t)}$ at an OSW, then directly detected at a PD and interpolated at a BPF to regenerate the desired radio signal. It is assumed that the code sequence $\mathrm{c_k(t)}$ matched with the one at the RBS is regenerated at the RCS, and the synchronization between two code sequences is taken. The radio signal, which is contaminated by all other radio signals, is fed into a demodulator in order to obtain the information data.

The radio signal $\mathrm{g_k(t)}$ at the kth RBS is represented by

$$g_k(t) = \mathrm{Re}\left[a_k(t)e^{j2\pi f_{rf}t}\right] \tag{1}$$

where $\mathrm{f_{rf}}$ is radio frequency and $\mathrm{a_k(t)}$ is the complex envelope with its bandwidth $\mathrm{B_{rf}}$. The optical on–off switching CDMA is performed at the OSW, driven by a code sequence $\mathrm{c_k(t)}$, whose frame period and chip width are $\mathrm{T_F}$ (second) and $\mathrm{T_c}$, respectively. Its pulse amplitude is one or zero. The intensity of the optical PAM/IM signal at the output of the OSW is given by

$$P_k(t) = P_s\left\{1 + g_k(t)\right\}c_k(t) \tag{2}$$

where $\mathrm{P_s}$ is the average transmitted optical power before optical switching.

$\mathrm{P_k(t)}$ is a bandpass natural sampled signal converted from a radio signal because an optical switching is a window-type sampling. Therefore, a radio signal can be conveyed by optical carrier while keeping its signaling format and regenerated from the pulsed signals by the interpolation at a BPF, if we choose a sampling period of less than or equal to half of the inverse of the radio signal bandwidth [$\leq 1/(2B_{rf})$]. Since a pseudorandom sequence is chosen as a code sequence that drives the OSW at the transmitter in the DOS-CDMA system, the durations between optical pulses become various values according to the kind of code sequence, but each pulse is surely repeated

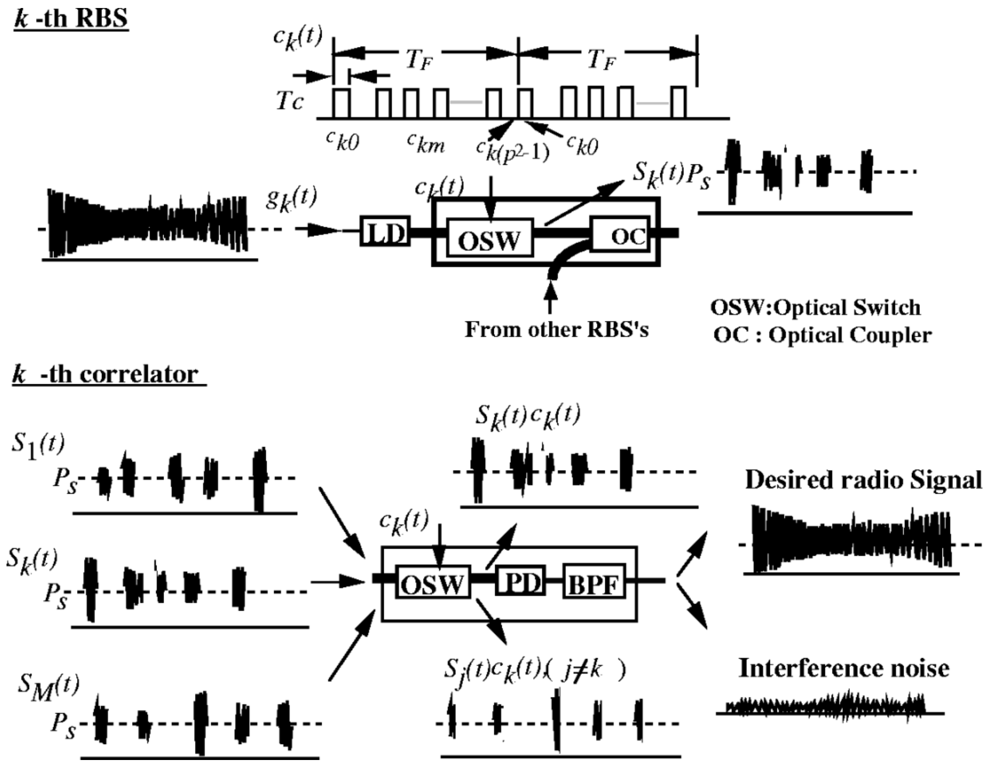

Fig. 2. Principle of DOS CDMA transmitter and receiver.

with its frame period of T_F. Therefore, in order to regenerate the radio signal after interpolation, T_F of less than or equal to $1/(2B_{rf})$ should be chosen. From the viewpoint of simplicity, however, using T_F of much less than $1/(2B_{rf})$ is not effective because a much faster speed for OSW is required. Hence, in this paper, T_F is set to be the maximum value, that is, $1/(2B_{rf})$.

To improve the quality of the regenerated radio signal in a DOS-CDMA system, a code sequence with the highest possible autocorrelation and the lowest possible cross-correlation has to be chosen. In the DOS-CDMA using optical IM/direct detection (DD) scheme, a unipolar code has to be used as a code sequence, while PN codes like maximum length code (M-sequence) or Gold code are used in a conventional radio CDMA system. Reference [20] reported that a prime code sequence is the best code as a unipolar orthogonal code that can provide the highest autocorrelation and the lowest cross-correlation of various orthogonal codes. Therefore, in the DOS-CDMA system, the prime code sequence is employed as a spread-spectrum (SS) code.

A set of prime codes has the preferable feature for an IM/DD CDMA system that there are very few coincidences of ones among code sequences. Prime codes with length p^2 are derived from prime sequences obtained from a Galois field GF(p) where p is a prime number. Table I shows an example of prime sequences and prime code sequences for a prime number p of seven. Each prime sequence element s_{mn} is obtained by the product of the corresponding m and m modulo p. Letting $c_m = (c_{m0}, c_{m1}, \ldots, c_{mj}, \ldots, c_{m(p-1)})$, denote the mth prime code sequence in which a jth code element c_{mj} is given by

$$c_{mj} = \begin{cases} 1, & j = s_{mn} + np \\ 0, & \text{otherwise.} \end{cases} \quad (3)$$

TABLE I
PRIME SEQUENCE AND PRIME CODE SEQUENCES FOR PRIME NUMBER

Prime sequences for p=7

m	s_{m0}	s_{m1}	s_{m2}	s_{m3}	s_{m4}	s_{m5}	s_{m6}
0	0	0	0	0	0	0	0
1	0	1	2	3	4	5	6
2	0	2	4	6	1	3	5
3	0	3	6	2	5	1	4
4	0	4	1	5	2	6	3
5	0	5	3	1	6	4	2
6	0	6	5	4	3	2	1

Prime code sequences for p=7

m	c_{m0}	c_{m1}	c_{m2}	c_{m3}	c_{m4}	c_{m5}	c_{m6}
0	1000000	1000000	1000000	1000000	1000000	1000000	1000000
1	1000000	0100000	0010000	0001000	0000100	0000010	0000001
2	1000000	0010000	0000100	0000001	0100000	0001000	0000010
3	1000000	0001000	0000001	0010000	0000010	0100000	0000100
4	1000000	0000100	0100000	0000010	0010000	0000001	0001000
5	1000000	0000010	0001000	0100000	0000001	0000100	0010000
6	1000000	0000001	0000010	0000100	0001000	0010000	0100000

In the DOS-CDMA scheme using prime codes, $T_F(= p^2 T_c)$ is set to $1/(2B_{rf})$ in order to gain the largest code length p^2 at the same switching speed of the OSW; thus the chip width T_c is given by T_F/p^2. When an OSW correlator is driven with the kth prime code sequence $c_k(t)$ at the receiver, the optical PAM/IM signal transmitted from the kth RBS is extracted out of all CDMA signals. Then the output current of the PD is composed of a desired signal component $S_k(t)$, interference components $I(t)$, and additive noise components $N(t)$. $S_k(t)$ and $I(t)$ are, respectively, given by

$$S_k(t) = \alpha P_r g_k(t) c_k(t) \quad (4)$$

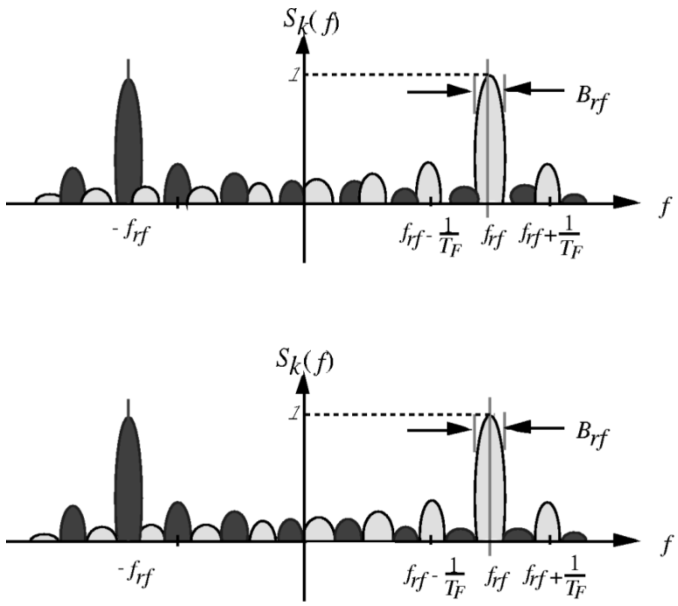

Fig. 3. Normalized both-side power spectrum density of signal. (a) Two components of desired signal and frequently are overlapped. (b) Two components of desired signal and frequently are not overlapped.

$$I(t) = \alpha P_r \sum_{j=1, j\neq k}^{M} g_j(t)c_j(t)c_k(t) \tag{5}$$

where α, $\mathrm{P_r}$, and M are the responsivity of the PD, the average received optical power at the correlator, and the total number of connected RBSs, respectively. Here, we derive the CIR in the DOS-CDMA system. We derive the power spectral density (PSD) of signal component $\mathrm{S_k(t)}$ by calculating the autocorrelation of $\mathrm{S_k(t)}$ from (4). The PSD of $\mathrm{S_k(t)}$, $\mathrm{S_k(f)}$, is given by

$$\begin{aligned} S_k(f) =& (\alpha P_r)^2 \frac{1}{p^2}\left(1+\frac{1}{p}-\frac{1}{p^2}\right) \\ &\times \left\{ G_k(f) + \frac{p-1}{p^2+p-1} \right. \\ &\left. \times \sum_{i=-\infty, i\neq 0}^{\infty} \mathrm{sinc}^2\left(\frac{\pi i}{p^2}\right) G_k(f-2iB_{rf}) \right\} \end{aligned} \tag{6}$$

where $\mathrm{G_k(f)}$ is the power spectrum of $\mathrm{g_k(t)}$ and $\mathrm{sinc(x)}$ is $\mathrm{sin(x)/x}$.

Fig. 3 shows the normalized both-sides PSD of the signal component. The first three terms of $\mathrm{S_k(f)}$ are the desired signal component around $\mathrm{f_{rf}}$ and $-\mathrm{f_{rf}}$, and the other terms are the frequency shifted components caused by bandpass sampling. Images of these shifted components cause the distortion in the desired signal as the self-interference if they overlap over the signal components as shown in Fig. 3(a). We can perfectly remove the self-interference components by setting the value of the radio frequency $\mathrm{f_{rf}}$ at $(j+1/2)B_{rf}$ or j/T_c (j is an integer) as shown in Fig. 3(b). Without such special values of $\mathrm{f_{rf}}$, however, the self-interference component may not deteriorate the signal quality because its power is low compared with that of the carrier signal component. We examine the carrier signal to self-interference power ratio (CSIR).

Fig. 4 shows some numerical results for the $\mathrm{f_{rf}}$ of 1.93 GHz and $\mathrm{B_{rf}}$ of 900 KHz. In the small p, the sinc function causes the up and down in CSIR, but as p increases, CSIR tends to be a saturated value of more than 30 dB, which is enough to obtain the radio signal quality in DOS-CDMA. As p increases, the saturated value of CSIR is determined by the relation between $\mathrm{f_{rf}}$ and $\mathrm{B_{rf}}$. Therefore, in the following analysis, we will ignore the self-interference components.

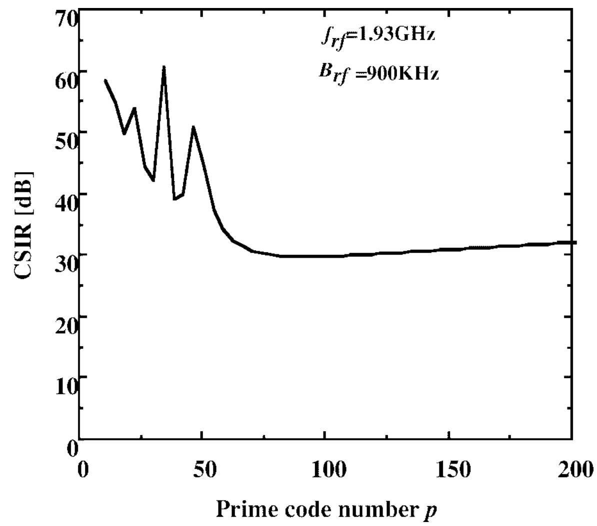

Fig. 4. Relationship between carrier to self-interference power ratio and prime code number p.

TABLE II
AVERAGE VARIANCE OF THE CROSS-CORRELATION OF THE PRIME CODE

p	$\sigma_c 2$
7	0.272
11	0.298
13	0.303
23	0.318
31	0.322
47	0.326
71	0.328
97	0.329

From (6), the carrier power of the regenerated radio signal $\mathrm{C_0}$ is given by

$$C_0 = (\alpha P_r)^2 \frac{1}{p^2}\left(1+\frac{1}{p}-\frac{1}{p^2}\right). \tag{7}$$

Let σ_c^2 denote the average variance of the cross-correlation of the prime code. Then, the carrier-to-interference power ratio $\mathrm{CIR_0}$ is given by

$$\mathrm{CIR_0} = \frac{p^2}{\sigma_c^2(M-1)}. \tag{8}$$

Table II shows σ_c^2 for different values of prime number p calculated by using computer simulation. σ_c^2 is a little increased as p increases but has a saturated value of 0.329 for $p=97$.

III. Optical Polarity Reversing Correlator (OPRC) for DOS-CDMA Using PN Codes

In the DOS-CDMA method described in Section II, only optical unipolar orthogonal codes such as prime codes [20] were applied to obtain a desired process gain because an optical switch is used to decode DOS-CDMA signals at each correlator. However, the prime code suffers a limit in the number of distinct

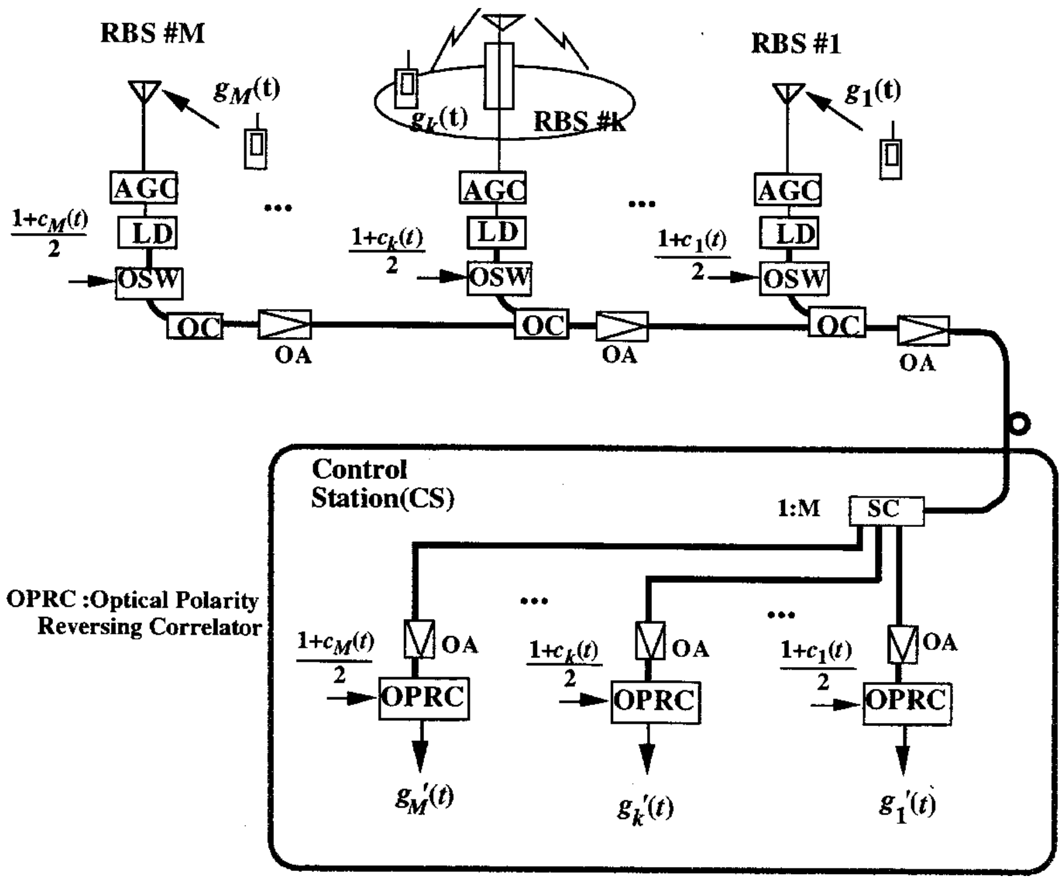

Fig. 5. Configuration of the DOS CDMA system.

code sequences, which results in the limitation of the number of radio base stations connected to the radio highway network. In addition, the use of prime codes for the DOS-CDMA scheme makes the optical power efficiency low because of its quite low pulse duty. Therefore, we should consider a new type of correlator for the DOS-CDMA method to which PN codes such as maximal length codes and gold codes can be applied because those codes are usually used in radio systems and generally superior in the number of distinct code sequences compared with prime codes. For digital networks using the optical CDMA method, the sequence inversion keyed (SIK) direct sequence (DS)-CDMA methods have been proposed in [26] and [27]. The method requires specially balanced PN codes. In order to allow the use of any unbalanced PN codes, the power splitting ratio of the power divider at the optical correlator has been controlled [28], and the transmission of two channels using two wavelengths or two orthogonal polarizations has been proposed [29]. In SIK-CDMA methods, however, binary digital data are encoded and transmitted with the positive polarity and the negative polarity of bipolar codes; thereby their correlators at the receiver cannot be applied to DOS-CDMA signals that are converted from radio signals by the on–off switching CDMA method. In this section, the OPRC for the DOS-CDMA radio highway network using PN codes [18], [30] is described.

Fig. 5 illustrates the configuration of the DOS-CDMA system with its topology of a bus-type fiber-optic link. M radio zones are connected to the bus link, where the radio signals from radio terminals in each zone are multiplexed by the DOS-CDMA scheme and transmitted to the RCS. The RBS in each zone equips only an LD, an OSW, and an automatic gain controller (AGC) and is connected to a bus link with a passive optical coupler (OC).

As mentioned in previous section, after the direct-intensity modulation of LD, the optical on–off switching SS is performed at the OSW, and in the bus-type fiber link, many optical signals are multiplexed by DOS-CDMA. At the receiver, the optical powers of the received DOS-CDMA signals from M RBSs are different from each other because the optical loss between each RBS and the RCS is different. Also, IM indexes of the received CDMA signals are different from each other because the radio signal received by the RBS has various amplitudes due to fading and different distance between terminals and a RBS. These differences cause the near–far problem in CDMA system. For this reason, an RBS is equipped with an AGC to control the amplitude of a received radio signal in order to keep the optical modulation index constant at the LD, and also equipped with an optical amplifier (OA) to compensate optical loss between two RBSs. At the RCS, optical CDMA signals from RBSs are at first power-split into each of M receivers, then received at the OPRC receiver.

A. Principle Of OPRC

The OPRC can be realized with various optical devices such as optical switches, matched filters, and Mach–Zehnder interferometers (MZIs). Fig. 6 illustrates the configuration of the transmitter and the OPRC for the optical CDMA using the PN code

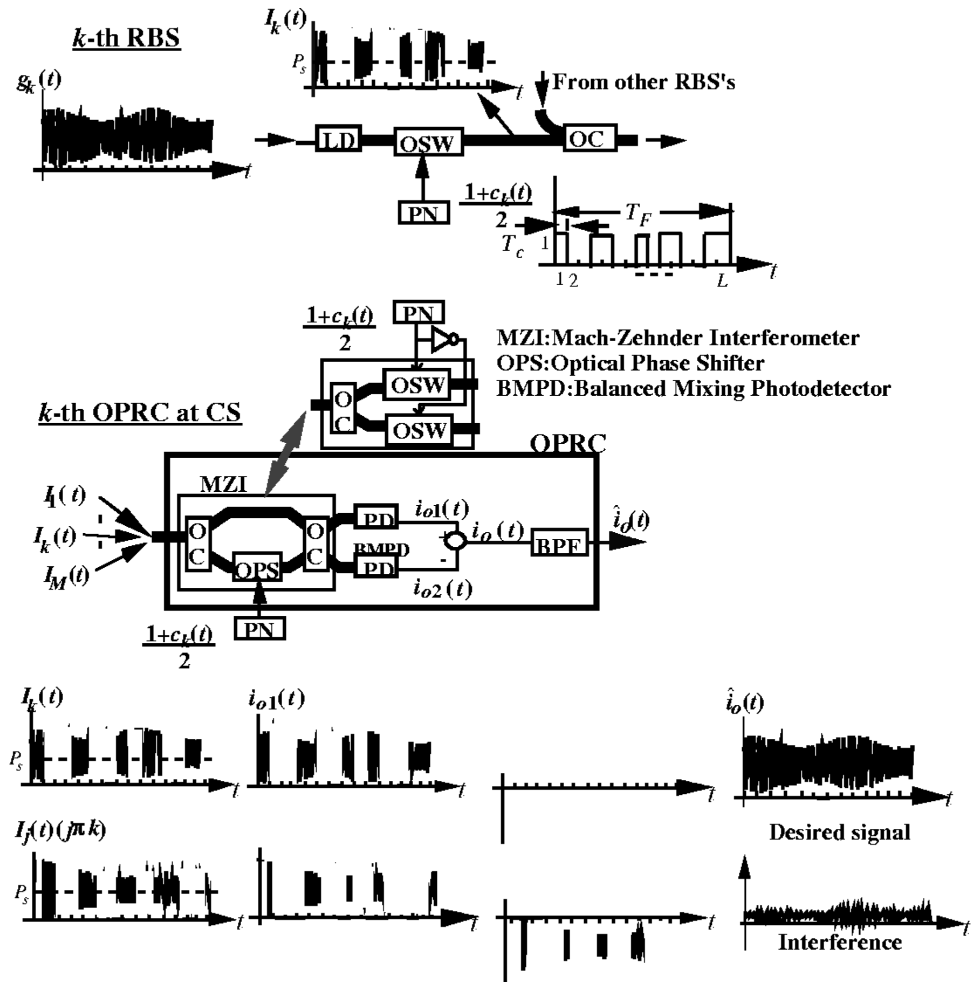

Fig. 6. Configuration of the transmitter and the OPRC receiver for DOS CDMA using PN codes.

$c_k(t)$ having the value of 1 or -1. The $c_k(t)$ has the frame period T_F and the chip width T_c. In the interval of T_F, $c_k(t)$ has the code length of L chips, and the number of weight ones is $(L+1)/2$. At the kth RBS, LD is assumed to be directly modulated by the radio signal with the optical modulation index of one. DOS-CDMA is performed by OSW driven with the biased PN code $c'_k(t) = (1 + c_k(t))/2$. Then, the intensity of optical signal from the kth RBS is written by

$$I_k(t) = P_s \{1 + g_k(t)\} c'_k(t) \tag{9}$$

where $g_k(t)$ is the radio signal with the bandwidth B_{rf} and the carrier frequency f_{rf}, and P_s is the average transmitted optical power before the optical switching.

At the kth OPRC, many IM/CDMA signals are received and split into two signals at the OC. It is assumed that the biased PN code $c'_k(t)$ matched with the one at the kth RBS is regenerated at the RCS by using the retiming code generator such as the retiming block, and the synchronization between two code sequences is taken. Then, the OPRC is driven by the biased PN code. In the case of the OPRC realized with an MZI, the phase of the optical phase shifter (OPS) is shifted according to the biased PN code $c'_k(t)$. When $c'_k(t)$ is one, the phase difference between both arms of MZI is zero, thus IM/CDMA signals are outputted to the upper port of MZI through the second OC. When $c'_k(t)$ is zero, the phase difference between both arms of MZI is set to π; thus the lower port of MZI outputs IM/CDMA signals through the second OC. In the case of OPRC realized with two OSWs, the upper OSW is set to "on" when $c'_k(t)$ is one, and the lower OSW is set to "on" when $c'_k(t)$ is zero. Thus, the output currents of the balanced mixing PD (BMPD) are expressed as

$$i_{o1}(t) = \alpha \sum_{j=1}^{M} P_{r_k} g_j(t) c'_j(t) c'_k(t) + i_{n1}(t) \tag{10}$$

$$i_{o2}(t) = \alpha \sum_{j=1}^{M} P_{r_k} g_j(t) c'_j(t) \frac{1 - c_k(t)}{2} + i_{n2}(t) \tag{11}$$

where α is the responsivity of the PD and $i_{n1}(t)$ and $i_{n2}(t)$ are additive noise currents, respectively. Equations (10) and (11) show that the positive polarity of the desired kth code $c_k(t)$ matches with the kth one at the RBS at the upper port of MZI or the upper OSW. However, it is obstructed at the lower port of MZI or the lower OSW. The desired kth signal at the input to the BPF is a bandpass natural sampled signal converted from the kth radio signal $g_k(t)$. The radio signal can be regenerated from the pulsed signals by the interpolation at the BPF, as discussed in Section II.

On the other hand, for the interference signal $I_j(t)(j \neq k)$, both ports of MZI or both OSWs generate interferences only when the positive polarity of $c_j(t)$ coincides with the positive or negative polarity of $c_k(t)$. Two interferences of BMPD are subtracted and suppressed at the BPF. However, in the unipolar-type correlator described in Section II-B, PN codes cannot be applied because the interference is never suppressed though the code sequence length increases. Details will be discussed in the next section.

B. Carrier-To-Interference Ratio Performance

The OPRC can be implemented instead of the unipolar-type correlator for a prime code at the receiver in DOS-CDMA system, as shown in Fig. 5. This section investigates the CINR performance improved by the OPRC for PN codes.

The carrier power C and the interference power I can be theoretically derived from the PSD of the output of BPF at the receiver by the same manner as Section II-B. The results are as follows:

$$C = \frac{1}{2}\left\{\frac{\alpha P_s(L+1)}{2L}\right\}^2 \tag{12}$$

$$I = \begin{cases} \frac{M-1}{2}\left(\frac{\alpha P_s}{2}\right)^2 \frac{L^2+5L+7}{4L^3}, & \text{for gold codes} \\ \frac{M-1}{2}\left(\frac{\alpha P_s}{2}\right)^2 \frac{(L+1)^2}{L^3}, & \text{for maximal length codes} \end{cases} \tag{13}$$

where P_s is the averaged received optical power. Hence, from (12) and (13), the CIRs for gold codes and maximal length codes are written by

$$\text{CIR} = \begin{cases} \frac{4}{M-1}\frac{L(L+1)^2}{L^2+5L+7} & \text{for gold codes} \\ \frac{L}{M-1} & \text{for maximal length codes.} \end{cases} \tag{14}$$

It is seen from (14) that the CIR is improved in proportion to the code length L. For comparison, we show the CIR in the case that PN codes are applied to the unipolar-type correlator as the same with the proposed OPRC. The CIR is written by

$$\text{CIR}_{uc} = \begin{cases} \frac{4}{M-1}\frac{4L(L+1)^2}{4L^3+17L^2+25L+15} & \text{for gold codes} \\ \frac{4}{M-1}\frac{L(L+1)^2}{L^3+5L^2+7L+3} & \text{for maximal length codes.} \end{cases} \tag{15}$$

It is seen from the comparison between (14) and (15) that the OPRC is effective for PN code, while the unipolar type correlator never improves the CIR for any L.

C. Numerical Results and Discussions

In this section, we show some numerical results and discussions. Parameters used for calculation are summarized in Table III. Fig. 7 shows the relationship between the code length L and the CIR for the OPRC shown in Fig. 6 and the unipolar-type correlator shown in Fig. 2 in the case of using PN codes for $M = 10$. In the case of the unipolar-type correlator using maximal length codes and gold codes, there is no improvement in the CIR though L increases. It is also seen from (15) that the CIR almost equals $4/(M-1)$ regardless of L. Hence, PN codes cannot be applied to the unipolar-type correlator. However, it is seen from Fig. 7 and (14) that in the OPRC, the CIR is improved as the L increases. The results show that PN codes such as maximal length codes and gold codes can be applied to the DOS-CDMA radio highway using the OPRC.

TABLE III
PARAMETER USED FOR CALCULATIONS

Responsivity of PD	α	0.8A/W
PSD of the relative intensity noise	ζ_{RIN}	-152dB/Hz
Bandwidth of optical filter	W	1THz
Noise temperature	T	300K
Load resistance	R_L	50 Ω
Spontaneous emission factor of OA	η_{sp}	2.0
Quantum efficiency of the OA	η_a	0.5
Radio signal frequency	f_{rf}	1.93GHz
Radio signal bandwidth	B_{rf}	900KHz
Coupling plus insertion loss of OC	L_{OC}	3dB
Fiber loss between RBS's	L_f	0.5dB
FWHM of the LD	$\Delta\nu_{LD}$	10MHz
Difference of center frequency of the LD	Δ_F	1THz

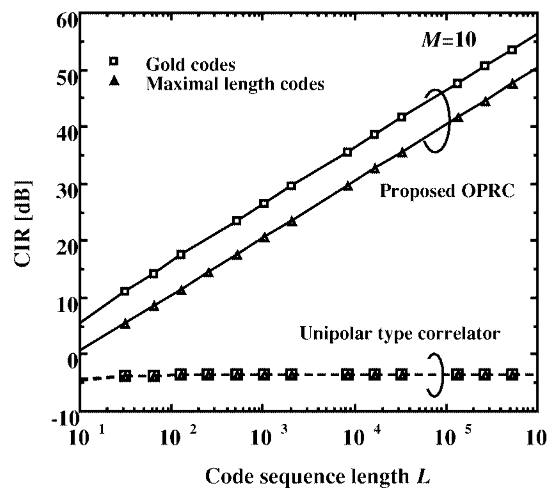

Fig. 7. Relationship between the code sequence length L and the CIR.

Reference [20] has reported that the prime code is the best as a unipolar orthogonal code that can provide the highest CIR. In the next figure, we compare the number of distinct code sequences that results in the limitation of the number of RBSs connected to the radio highway for maximal length codes, gold codes, and prime codes. Fig. 8 shows the number of distinct code sequences versus the code sequence length L. Gold code sequences are generated by combining a pair of preferred maximal length sequences using modulo-2 addition if the number of preferred maximal length sequences is at least two [31]. On the other hand, in the case of prime codes, the number of distinct code sequences is equal to the prime number p for the code sequence length of p^2. The numbers of distinct code sequences for maximal length codes and gold codes are larger than that for prime codes. For example, comparing maximal length codes and gold codes of $L = 32\,767$ with prime codes of $p^2 = 32\,041$, the numbers of distinct code sequences for maximal length codes and gold codes are ten times and 183 times larger than that for prime codes, respectively. Therefore, using the proposed OPRC can assign a larger number of distinct code sequences to RBSs in optical CDMA radio highway than using the unipolar-type correlator using prime codes.

Fig. 9 shows the relationship between the switching speed $1/T_c$ and the number of maximum connected RBSs M_{max} in

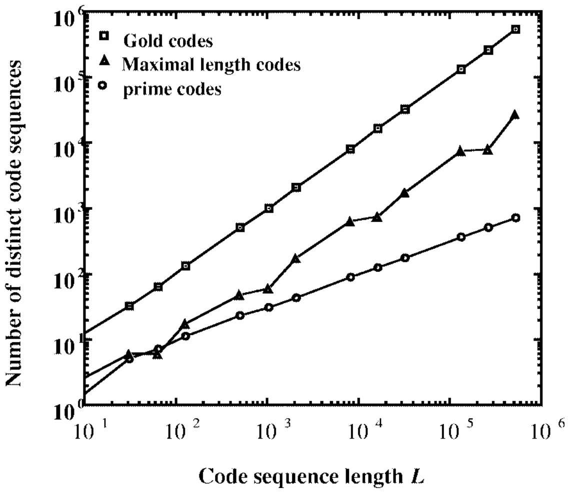

Fig. 8. Number of distinct code sequences versus the code sequence length L.

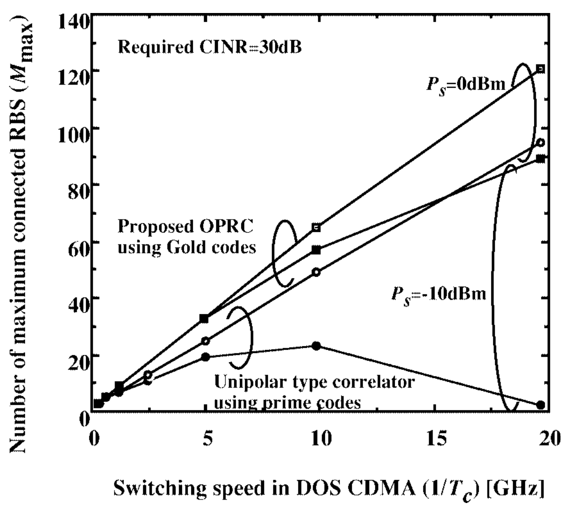

Fig. 9. Relationship between the switching speed in the DOS-CDMA and the number of maximum connected RBSs.

the case that the required CINR is 30 dB. The CINR is analyzed assuming the exist of the receiver thermal noise, the relative intensity noise, and the spontaneous emission noise of OA. This figure shows that by the OPRC using Gold codes, the number of maximum connected RBSs can be much further improved for small P_s such as -10 dBm compared with the unipolar-type correlator for prime codes—for example, in the case of $1/T_c = 9.8$ GHz, which corresponds to a code length of about 5440. The switching speed can be realized by the available state-of-the-art switch. The proposed OPRC using gold codes can accommodate 1.3 and 2.5 times the number of RBSs to the radio highway with a CINR of 30 dB compared with the unipolar-type correlator using prime codes for P_s of 0 dBm and -10 dBm, respectively. In this analysis, however, the switching waveform and the extinction ratio of OSW are assumed to be ideal rectangular and infinity, respectively. The evaluation of the influence from their degradation should be a further subject.

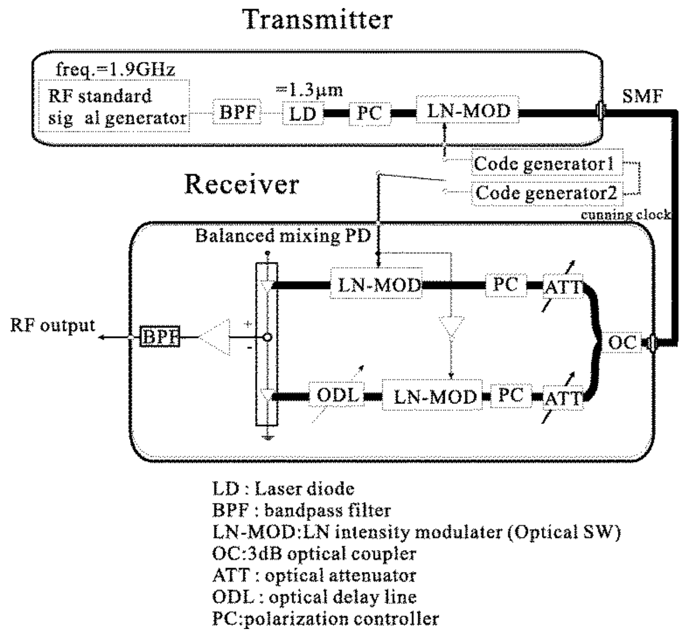

Fig. 10. Experimental setup for DOS-CDMA using OPRC receiver.

TABLE IV
SPECIFICATIONS OF EXPERIMENTAL SETUP

LD module (ORTEL 3541C)	DFB Laser wavelength λ : 1.3μm output power : 3.4dBm RIN : -149dB/Hz efficiency γ : 0.103W/A
LN intensity modulator (in transmitter) (RAMAR corp.)	insertion loss : 6.1 dB extinction ratio : 35.7 dB Vπ : 6.0 V
LN intensity modulator (in receiver) (Sumitomo TMZ1.3-2.5)	insertion loss: 6.0 (upp.), 4.4(low.) dB extinction ratio : 33.2 (upp.), 32.0 (low.) dB Vπ : 1.2 (upp.), 1.0(low.) V
PD(NEC NDL5481P1)	sensitivity : 0.91 A/W
RF modulation RF carrier frequency	π/4 shift DQPSK 1.9 GHz
input RF power	10 dBm
chip rate of M-sequence code length	4.2 Mcps 7~2047
RF bandwidth	300 kHz

IV. AN EXPERIMENTAL INVESTIGATION OF INTERFERENCE SUPPRESSION IN OPRC

This section shows the experimental investigation of CIR performance in DOS-CDMA system. We will experimentally show the CIR performance improved by using OPRC compared to using the unipolar-type correlator. We will also observe for the first time that the CIR performance is further improved by using the even weight maximal length code compared to using the odd weight maximal length code.

Fig. 10 shows the experimental setup, the specifications of which are summarized in Table IV [32]. The transmitter consists of LD and $LiNbO_3$ intensity modulator (LN-MOD). The RF signal intensity-modulates the LD with its wavelength of 1.3 μm. The IM signal is on–off encoded at the LN-MOD driven

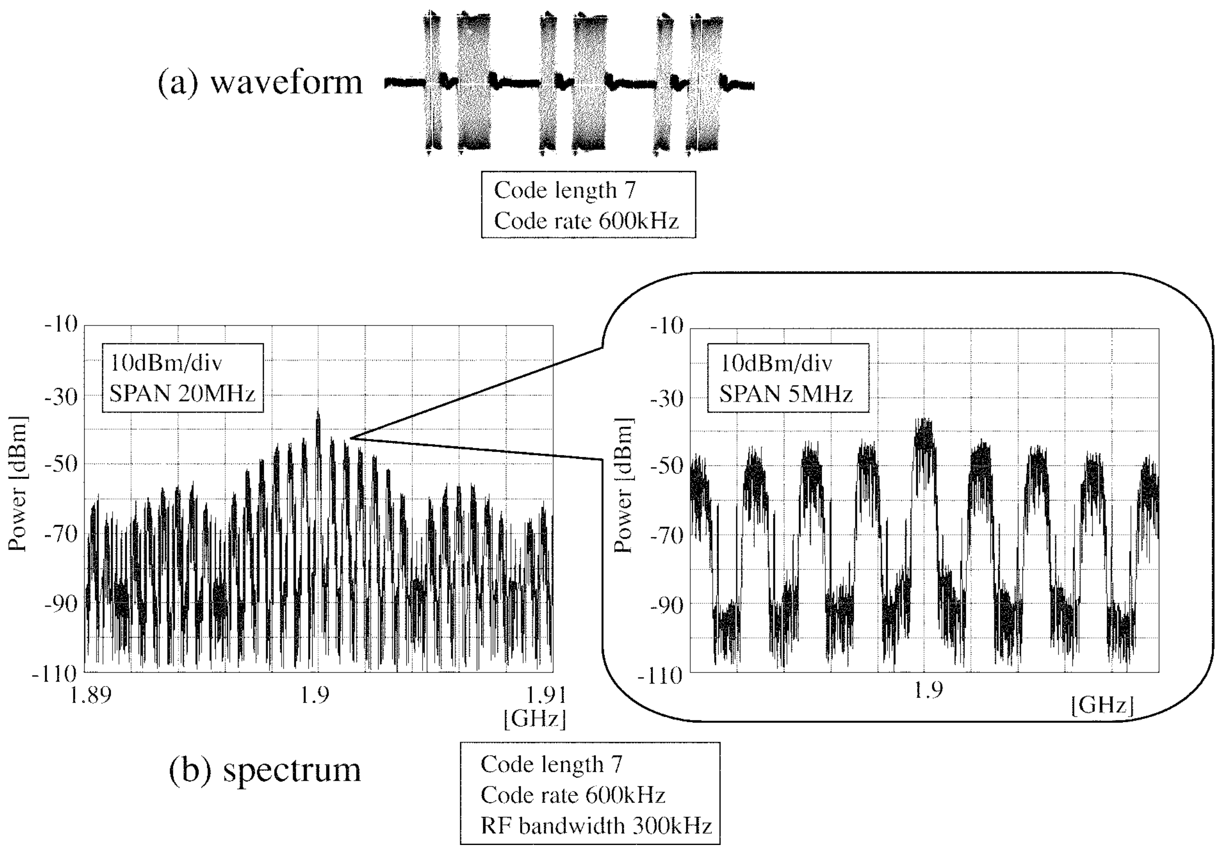

Fig. 11. Waveform and spectrum of DOS-CDMA signal at the output of the transmitter: (a) the waveform and (b) its spectrum.

with the rectangular pulsed M-sequence from the code generator. The receiver consists of a 3-dB coupler, two LN-MODs, an optical delay line (ODL), two optical attenuators (ATTs), a BMPD, a BPF, and an RF amplifier.

At the receiver, the received optical signal is divided into two branches by a 3-dB coupler. The divided optical signals are decoded at each LN-MOD. The LN-MOD in the upper branch is driven with the biased PN code $(1-c_k(t))/2$, and the LN-MOD in the lower branch is driven with $(1+c_k(t))/2$, that is inverse one of the input M-sequence. At the BMPD, the decoded optical signals are photodetected and subtracted. The output of the BMPD is the pulsed RF signal, and the interpolation of the BPF regenerates the desired RF signal and at the same time suppresses the interference signal.

Fig. 11(a) shows an example of the waveform of the transmitter output in the case of a code length of seven and a code rate of 600 kHz. We can see that the PN pattern is mapped into an RF intensity-modulating signal. Fig. 11(b) shows an example of the spectrum of the transmitter output in the case of radio signal bandwidth of 300 kHz. The spectrum has a symmetric sinc type about the center frequency of 1.9 GHz and the harmonic components appear at intervals of the code frequency 300 kHz.

Next, we measured the CINR performance of OPRC for DOS-CDMA. The desired RF signal power was measured when the transmitter and the receiver use the same maximal length code. Code synchronization between the transmitter and receiver was obtained by using cunning clock. The interference RF power was measured when the receiver used a chip-shifted maximal length code as a code different from the desired one.

Fig. 12 shows the experimental result of the relationship between the code length versus CINR performance in the case of the chip rate of 4.2 Mchips/s. In this figure, "w/o OPRC" means to use the unipolar-type correlator. We can observe the CINR improvement. This improvement is caused by CIR improvement obtained by the OPRC receiver. The OPRC can improve CIR in proportion to the square of code length, while the increase of the code length never improves the CIR performance in the case of the use of the unipolar-type correlator. The CINR value was around 6 dB.

When we use bipolar PN codes having a value of 1 or -1 as spreading codes of DOS-CDMA system, there are two methods in code mapping into optical on–off pulses. One is to map weight "1" of the code into optical on-pulse, and another is to map the weight "-1" of the code into optical on-pulses. However, the number of on-pulses in a DOS-CDMA signal becomes different between these two methods, because the numbers of the "1" and "-1" weight of bipolar codes such as maximal length code, gold code, and so on, are ordinarily different. This fact leads to the difference in the obtained CIR. A code from maximal length codes has even weight "-1" and odd weight "-1," and the number of odd weight "-1" is larger than that of even weight "-1." In this experiment using maximal length code, the former is called the even weight maximal length code and the latter is called the odd weight

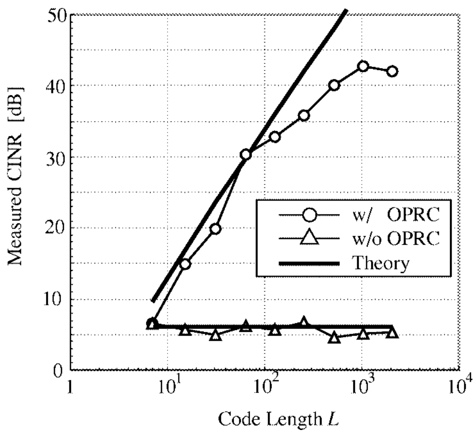

Fig. 12. Measured CINR performance versus the code length of PN code.

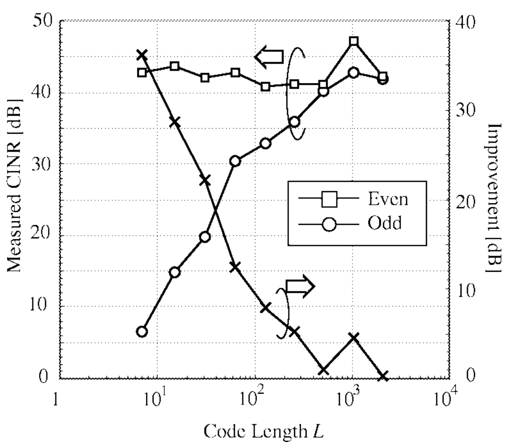

Fig. 13. Measured CINR performance in using the even weight maximum length code and its improvement.

maximal length code. In the experimental results shown in Fig. 12, we used the odd weight maximal length code at the encoder of the transmitter as in the analysis in Sections II and III, because it made the received optical power as large as possible. However, the obtained CIR should be examined when using the even weight maximal length code, because it will be much easier to make the interference RF power between upper and lower branches at the OPRC quite the same.

Fig. 13 shows the measured CINR performance versus code length for the even and odd weight maximal length code in the case of the chip rate of 4.2 Mchips/s. While CINR is improved as the code length increasing for the odd weight maximal length code, the CINR for the even weight maximal length code has a fixed value of about 42 dB for any value of the code length, which is dominated by the noise power. Compared with the odd weight maximal length code, the improvement in CINR obtained by the even weight M-sequence is about 35 and 10 dB for code lengths of 7 and 127 chips, respectively.

V. SUMMARY

Radio highway networks enable us to operate more flexible radio air interfaces. Therefore, we can use a variety of frequency bands without replacing the base station equipment and networks. We have proposed DOS-CDMA method for the radio highway network and investigated its performance. Theoretical and experimental results have shown that the proposed OPRC is effective for DOS-CDMA system using conventional bipolar PN code and also confirmed the availability of the application of the even weight maximal length code for DOS-CDMA system.

ACKNOWLEDGMENT

The authors are thankful to Prof. S.-J. Park, Seowon University, Korea, for his invaluable support.

REFERENCES

[1] H. Harada, K. Sato, and M. Fujise, "A feasibility study on a radio-on-fiber based road-to-vehicle communication systems by a code division multiplexing radio transmission scheme," in *Proc. ITST2000*, Oct. 2000, pp. 155–160.

[2] K. Morita and H. Ohtsuka, "The new generation of wireless communications based on fiber-radio technologies," *IEICE Trans. Commun.*, vol. E76-B2, no. 9, pp. 1061–1068, Sept. 1993.

[3] Y. Okada, N. Hirakata, A. Kamemura, T. Saito, Y. Masuda, and Y. Koshino, "Optical fiber link radio expansion system for weak reception area," in *Proc. ICUPC'95*, Tokyo, Japan, Nov. 1995, pp. 501–505.

[4] Y. Ebine, "Development of fiber-radio systems for cellular mobile communications," in *Tech. Dig. MWP'99*, Melbourne, Australia, Nov. 1999, pp. 249–252.

[5] I. Seto *et al.*, "Small-size remote base station with radio-over-fiber (ROF) techniques for IMT-2000," in *Tech. Dig. 4th KJWS on MMWP*, Daejeon, Korea, Jan. 2003, pp. 9–12.

[6] W. I. Way, "Subcarrier multiplexed lightwave system design considerations for subcarrier loop applications," *J. Lightwave Technol.*, vol. 7, pp. 1806–1818, Nov. 1989.

[7] S. Komaki, K. Tsukamoto, S. Hara, and N. Morinaga, "Proposal of fiber and radio extension link for future personal communications," *Microwave Opt. Technol. Lett.*, vol. 6, no. 1, pp. 55–60, Jan. 1993.

[8] J. Namiki *et al.*, "Optical feeder basic system design for microcellular mobile radio," *IEICE Trans. Commun.*, vol. E76-B, no. 9, pp. 1069–1077, Sept. 1993.

[9] H. Ogawa *et al.*, "Microwave and millimeter-wave fiber optic technologies for subcarrier transmission systems," *IEICE Trans. Commun.*, vol. E76-B, no. 9, pp. 1078–1090, Sept. 1993.

[10] W. I. Way, "Optical fiber-based microcellular systems: an overview," *IEICE Trans. Commun.*, vol. E76-B, no. 9, pp. 1091–1102, Sept. 1993.

[11] S. Komaki, K. Tsukamoto, M. Okada, and H. Harada, "Proposal of radio highway networks for future multimedia-personal wireless communications," in *Proc. ICPWC'94*, Aug. 1994, pp. 204–208.

[12] S. Komaki, K. Tsukamoto, and M. Okada, "Requirements for radio-wave photonic devices from the viewpoint of future mobile radio systems," *IEEE Trans. Microwave Theory Tech.*, vol. 43, pp. 2222–2228, Sept. 1995.

[13] T. H. Wood and N. K. Shankaranarayanan, "Operation of a passive optical network with subcarrier multiplexing in the presence of optical beat interference," *J. Lightwave Technol.*, vol. 11, pp. 1632–1640, Oct. 1993.

[14] H. Harada, K. Tsukamoto, S. Komaki, and N. Morinaga, "Optical TDMA scheme for fiber-optic millimeter-wave radio system," *Trans. IEICE Jpn.*, vol. J77-C-I, no. 11, pp. 649–658, Nov. 1994.

[15] H. Harada, S. Kajiya, K. Tsukamoto, and S. Komaki, "TDM intercell connection fiber-optic bus link for personal radio communication systems," *IEICE Trans. Commun.*, vol. E78-B, no. 9, pp. 1287–1294, Sep. 1995.

[16] M. M. Banat and M. Kavehrad, "Reduction of optical beat interference in SCM/WDM networks using pseudorandom phase modulation," *J. Lightwave Technol.*, vol. 12, pp. 1863–1868, Oct. 1994.

[17] S. J. Park, K. Tsukamoto, and S. Komaki, "Proposal of direct optical switching CDMA for cable-to-the-air system and its performance analysis," *IEICE Trans. Commun.*, vol. E81-B, no. 6, pp. 1188–1196, June 1998.

[18] ——, "Polarity-reversing type photonic receiving scheme for optical CDMA signal in radio highway," *IEICE Trans. Electron.*, vol. E81-C, no. 3, pp. 462–467, March 1998.

[19] S. Kajiya, K. Tsukamoto, and S. Komaki, "Proposal of fiber-optic radio highway networks using CDMA method," *IEICE Trans. Electron.*, vol. E79-C, no. 1, pp. 111–117, Jan. 1996.

[20] P. R. Prucnal, M. A. Santoro, and T. R. Fan, "Spread spectrum fiber-optic local area network using optical processing," *J. Lightwave Technol.*, vol. LT-4, pp. 547–554, May 1986.

[21] J. A. Salehi, A. M. Weiner, and J. P. Heritage, "Coherent ultrashort light pulse code-division multiple access communication systems," *J. Lightwave Technol.*, vol. 7, pp. 478–491, Mar. 1990.

[22] S. Benedetto and G. Olmo, "Performance evaluation of coherent optical CDMA," *Electron. Lett.*, vol. 27, no. 22, pp. 2000–2002, Oct. 1991.

[23] J. A. Salehi, "Code division multiple access techniques in optical fiber networks—Parts I: fundamental principles," *IEEE Trans. Commun.*, vol. E37, no. 8, pp. 824–833, Aug. 1989.

[24] T. L. Duffield, "A comparison of modulation techniques for quantized voice communications," *IEEE Trans. Commun.*, vol. COM-18, pp. 543–550, Oct. 1970.

[25] A. Kohlenberg, "Exact interpolation of band-limited functions," *J. Appl. Phys.*, vol. 12, no. 12, pp. 1432–1436, Dec. 1953.

[26] T. O'Farrell and S. I. Lochmann, "Performance analysis of an optical correlator receiver for SIK DS-CDMA communication systems," *Electron. Lett.*, vol. 30, no. 1, pp. 63–65, Jan. 1994.

[27] ——, "Switched correlator receiver architecture for optical CDMA networks with bipolar capacity," *Electron. Lett.*, vol. 31, no. 11, pp. 905–906, May 1995.

[28] F. Khaleghi and M. Kavehrad, "A new correlator receiver architecture for noncoherent optical CDMA networks with bipolar capacity," *IEEE Trans. Commun.*, vol. 44, pp. 1335–1339, Oct. 1996.

[29] L. Nguyen, B. Aazhang, and J. F. Young, "All-optical CDMA with bipolar codes," *Electron. Lett.*, vol. 31, no. 6, pp. 469–470, Mar. 1995.

[30] S. J. Park, K. Tsukamoto, and S. Komaki, "Proposal of radio highway network using a novel direct optical switched CDMA method," in *Tech. Dig. MWP'96*, Kyoto, Japan, Dec. 1996, pp. 77–80.

[31] S. Tamura, S. Nakano, and K. Okazaki, "Optical code-multiplex transmission by Gold sequence," *J. Lightwave Technol.*, vol. LT-3, pp. 121–127, Feb. 1985.

[32] T. Higashino, K. Tsukamoto, and S. Komaki, "Experimental study of received signal performance in direct optical switching CDMA ROF system," in *Tech. Dig. MWP2002*, Hyogo, Japan, Nov. 2002, pp. 233–236.

Katsutoshi Tsukamoto (M'88) was born in Shiga, Japan, on October 7, 1959. He received the B.E., M.E., and Ph.D. degrees in communications engineering from Osaka University, Osaka, Japan, in 1982, 1984, and 1995, respectively.

He is currently an Associate Professor in the Department of Communications Engineering, Osaka University, engaging in research on radio and optical communication systems.

Prof. Tsukamoto is a Member of the Institute of Electronics and Information Communication Engineers (IEICE) of Japan and the Institute of Television Engineers of Japan. He received the Paper Award from the IEICE in 1996.

Takeshi Higashino was born in Osaka, Japan, on November 11, 1978. He received the B.E. and M.E. degrees in communications engineering from Osaka University, Osaka, Japan, in 2001 and 2002, respectively, where he is currently working toward the Ph.D. degree.

He is engaging in research on radio and optical communication systems.

Takashi Nakanishi was born in Hyogo, Japan, on September 12, 1979. He received the B.E. degree in communications engineering from Osaka University, Osaka, Japan, in 2002, where he is currently working toward the M.E. degree.

He is engaged in research on radio and optical communication systems.

Shozo Komaki (M'84–SM'94) was born in Osaka, Japan, in 1947. He received the B.E., M.E., and Ph.D. degrees in electrical communication engineering from Osaka University, Osaka, Japan, in 1970, 1972, and 1983, respectively.

In 1972, he joined NTT Radio Communication Laboratories, where he was engaged in repeater development for a 20-GHz digital radio system, 16-QAM, and 256-QAM systems. In 1990, he joined the Faculty of Engineering, Osaka University, engaging in research on radio and optical communication systems. He is currently a Professor at Osaka University.

Prof. Komaki is a Member of the Institute of Electronics and Information Communication Engineers (IEICE) of Japan and the Institute of Television Engineers of Japan. He received the Paper Award and the Achievement Award from IEICE in 1977 and 1994, respectively.